

# Evaluation of Geo-hazard Induced by Zarand Earthquake in Central Iran Using Thermal Remote Sensing Data and GIS



Hamid Allahvirdiasl, Himan Shahabi, Ayub Mohammadi, Ataollah Shirzadi, Wei Chen, Mehdi Ahmadi, and Masood Khodadadi

**Abstract** Land degradation is one of the environmental hazards that can occur in most countries during the last century. Geo-hazards induced by earthquakes have caused environmental degradation. Inevitably, stresses occurring prior to an earthquake in tectonically active places are able to boost the near-ground temperature of a region. Thermal remote sensing can usually detect these transformations, which can provide substantial clues about future earthquakes. The aim of this study is to analyze land surface temperature (LST) variations due to the Zarand Earthquake,

---

H. Allahvirdiasl

Faculty of Built Environment and Surveying, Universiti Teknologi Malaysia (UTM), 81310 Johor Bahru, Malaysia

e-mail: [p\\_hamid84@yahoo.com](mailto:p_hamid84@yahoo.com)

H. Shahabi (✉)

Department of Geomorphology, Faculty of Natural Resources, University of Kurdistan, Sanandaj, Iran

e-mail: [h.shahabi@uok.ac.ir](mailto:h.shahabi@uok.ac.ir)

A. Mohammadi

Department of Remote Sensing and GIS, University of Tabriz, 51666-16471 Tabriz, Iran

e-mail: [mohammadi.ayub@tabrizu.ac.ir](mailto:mohammadi.ayub@tabrizu.ac.ir)

A. Shirzadi

Department of Rangeland and Watershed Management, Faculty of Natural Resources, University of Kurdistan, Sanandaj, Iran

e-mail: [a.shirzadi@uok.ac.ir](mailto:a.shirzadi@uok.ac.ir)

W. Chen

College of Geology & Environment, Xi'an University of Science and Technology, Xi'an 710054, China

e-mail: [chenwei0930@xust.edu.cn](mailto:chenwei0930@xust.edu.cn)

M. Ahmadi

Department of Geomorphology, Faculty of Planning and Environmental Sciences, University of Tabriz, 51666-16471 Tabriz, Iran

M. Khodadadi

School of Business and Creative Industries, University of the West of Scotland, Paisley PA1 2BE, UK

e-mail: [masood.khodadadi@uws.ac.uk](mailto:masood.khodadadi@uws.ac.uk)

© The Author(s), under exclusive license to Springer Nature Switzerland AG 2022

A. M. F. Al-Quraishi et al. (eds.), *Environmental Degradation in Asia*,

Earth and Environmental Sciences Library,

[https://doi.org/10.1007/978-3-031-12112-8\\_4](https://doi.org/10.1007/978-3-031-12112-8_4)

which occurred in south–central Iran during 10–28 February 2005, by using the MODIS LST product. In addition, ten and six years of air temperature anomaly average data from before and after the Zarand earthquake, respectively, were used in this study. The results showed that the LST on 16th February was 28 °C, while on 21st February was 37 °C. Therefore, there was an LST difference of about 9 °C between both dates, so that there was a temporary abnormal rise in temperature before the earthquake occurred. On the other hand, the time series analysis of LST maps from 10 to 28th February 2005 showed that anomalies started six days before the main shock. Also, based on the correlation of MODIS LST and in-situ air temperature, interestingly, either the LST or air temperature started to rise on 16 February, or both soared on 21st February 2005.

**Keywords** Earthquake · Land surface temperature · Thermal remote sensing · Environmental degradation · Central Iran

## 1 Introduction

Earthquakes as one of environmental degradation is a major problem worldwide, especially in developing countries [1, 2]. With the increase in economic development, much more serious economic and social damage can be caused by unexpected earthquakes than ever before [3, 4]. Therefore, monitoring and studying of natural catastrophes, such as flood [5, 6], wildfire [7, 8], sinkhole [9], droughtiness [10], landslide [11], gully erosion [12], land cover [13], land/ground subsidence [14], groundwater [15], and earthquake [16] presents a severe scientific challenge [17]. Clearly, one of the most effective ways of minimizing the earthquakes' effects is predicting the event before it occurs, so that necessary measures can be taken to evacuate and warn those in danger [18]. Furthermore, understanding temperature anomalies in the land associated with earthquakes can help predict the earthquake and reduce the extreme earthquake impacts. The anomaly can be observed within two weeks up to few hours before the earthquake [19].

Ouzounov and Freund [20] proposed a mechanism to explain the temperature rise preceding an earthquake is the presence of positive hole-type charge carriers in rocks. LST as an important factor in investigating the temperature of areas close to the epicenter can provide new attitudes to study this catastrophic phenomenon [21]. This temperature difference is quite obvious in temperatures obtained from satellite images estimated from the Earth's emission information and from instruments placed 1.5 m above the ground, collecting air temperature data [22]. The observed thermal anomalies are related to the strong interaction between the lithosphere and atmosphere [23].

Satellite thermal infrared (TIR) imaging data show not only long-lived thermal fields associated with large fault systems and linear structures in the Earth's crust [24], but also short-lived anomalies prior to major earthquakes [25]. The short-lived anomalies in the land typically appear 7–14 days before an earthquake.

Recently, several techniques, including co-registration and geo-referencing of all relevant imagery from GOES and AVHRR have been developed to analyze satellite TIR imagery to identify anomalies [26]. Furthermore, other applied techniques are single image comparison of pre- versus post-earthquake TIR imageries, multispectral infrared component analysis of the MODIS Terra and Aqua data by using LST [20], and an analysis of pixel temperature variance from long-term scene threshold temperatures to identify “hot” areas [26].

Some researchers have also observed anomalies from two weeks to a few hours before the event at distances of 200–1000 km from the epicenter (China, Japan, Russia, Turkey, Chile, Mexico, and Greece) [27–30]. In addition, there are several satellite-based methods that show potential precursors to earthquakes [22]. It is worth mentioning that remote sensing has proved to be a useful tool for observing LST variations. Therefore, understanding the near real-time and large spatial scale LST variations from remote sensing images is of great importance because this domain has not been thoroughly explored, and it may provide valuable information for seismic studies in tectonically-active areas.

A change in the thermal regime of an epicenter region is one of the most striking changes and can be detected by space-borne sensors such as AVHRR and MODIS [31, 32]. Several studies have shown that numerous geophysical parameters are strongly related to earthquakes. If changes can be recognized before the earthquake, these parameters may be possible precursors of an earthquake occurrence. In particular, one of these parameters is LST, which can change before the earthquake. If LST anomalies before an earthquake could be observed, the prediction of earthquakes may be possible. Therefore, this research may make a valuable contribution to reducing the damage to the environment and manmade infrastructure and loss of life. This study will also be important to scientists who work on seismic research or research related to seismic activity.

In-situ air temperature data were used to show the increasing air temperature variation associated with the earthquake. Moreover, LST variation maps were produced from satellite data to show the temperature anomaly associated with the earthquake. Additionally, LST maps for the years 2004 and 2007 were produced to compare with 2005 (10th–28th February). Furthermore, this study covered the variation of LST that happened prior to the earthquake. The study area is the Zarand district earthquake in Kerman Province. The earthquake occurred on 22nd February 2005, with a magnitude of 6.4. However, the particular dates were 10th to 28th February 2005. The earthquake prediction is a challenging task to reduce the earthquake impact and hence reduce the damage by taking necessary precautions.

In this study, geo-hazard evaluation of Zarand Earthquake in central Iran, which occurred during 10th–28th February 2005, is analyzed and the land surface temperature (LST) variation for the years 2004, 2005, and 2007 are mapped. Finally, the in-situ air temperature variation for the entire month of February 2005 (1st–28th February) is analyzed and compared with data from the ten years before (1994–2004) and six years (2006–2011) after the earthquake. In this study, the satellite data utilized were the MODIS daytime LST product (MOD11A1) from the thermal band for 10th to 28th February 2005.

## 2 Study Area

The study area is located in Zarand district, Kerman Province, central Iran. On 22 February 2005 at 05:55 local time (02:25 GMT), an earthquake with a magnitude of 6.4 on the Richter scale struck the area. The epicenter was identified at 30.726 N, 56.817 E at a depth of 42 km at 55 km north-west of Kerman. The earthquake lasted for 12 s, caused extensive damage to the rural areas in Ravar district and Kerman district, and was much more disastrous for the Zarand district. More than 50 villages suffered between 30 and 100% damage as a consequence of this earthquake. Almost 612 were killed and 15,000 were injured. The population adversely affected is around 32,000 (Fig. 1). A great proportion of the population in several villages was severely affected due to poor building conditions.

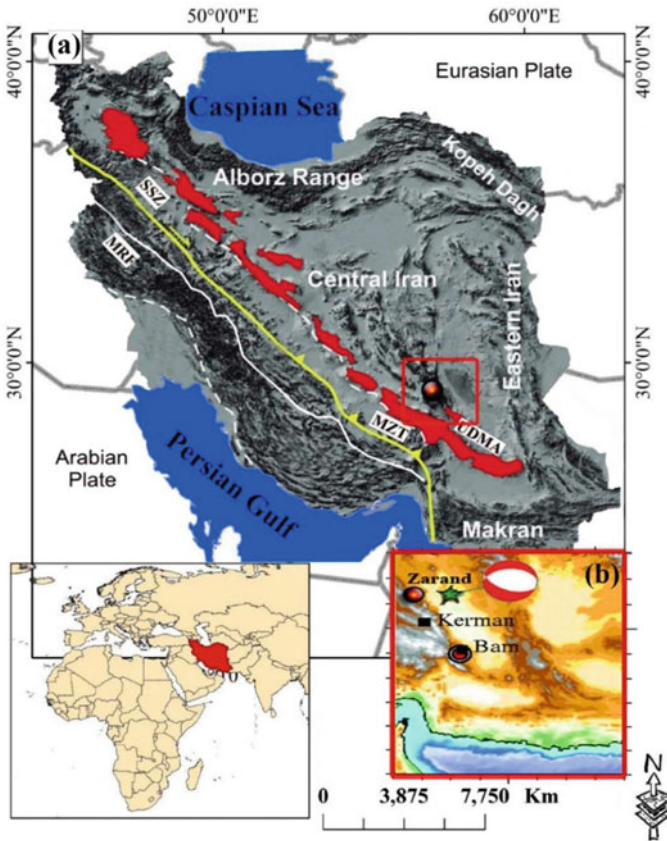


**Fig. 1** The geographical position of the study area in Iran; **a** structural units and tectonic features of the Arabia-Eurasia collision zone in Iran: SSZ (Sanandaj-Sirjan Zone), MRF (Main Recent Fault), MZT (Main Zagros Thrust), UDMA (Urumieh-Dokhtar Magmatic Arc); **b** geographical location of Zarand earthquake

The study area is based on the geological structure, is located between two tectonic units—the Urumieh-Dokhtar Magmatic Arc (UDMA) and Main Zagros thrust (MZT) [33]. The UDMA is situated between the Sanandaj-Sirjan Zone (SSZ) and central Iran, running parallel to the Zagros Mountains and the SSZ (Fig. 1a) [34].

### 3 Materials and Method

#### 3.1 Satellite Data Acquisition

MODIS was launched by NASA with on-board polar orbiting. This study used MODIS Terra because moderate-resolution remote sensing provides a way to quantify land surface characteristics such as snow cover extent, land cover type and extent, leaf area index, surface temperature, and fire occurrence. The MODIS Terra satellite launched on December 18th, 1999. It has 705 km orbit and descending node in which the local time is 10:30 A.M. It has sun-synchronous, near-polar orbiting. The swath angle for this satellite is 2330 km (cross track) by 10° of latitude (along track) [35]. In addition, it has 36 bands with spatial resolutions of 250 m for bands 1–2, 500 m for bands 3–7, and 1000 m for bands 8–36 [36].

The data used for this research was MODIS Terra Land level 3 Daily Tiled LST Products (MOD11A1 Level 3 Daily Land Surface Temperature/Emissivity-1 km). The spatial resolutions for applied Aqua MODIS data for the current study are 1 and 5 km. The source of the data was through this website (<http://ladsweb.nascom.nasa.gov/>).

#### 3.2 Satellite Data Analysis

Needless to say, high-resolution LST is usually derived from thermal infrared satellite observations using a multi-channel technique. In general, surface-emitted TIR radiance depends on its temperature and emissivity, varying with the wavelength. In the current study, 19 images have been used to analyze the temperature variation in 2005. The images which have been downloaded are as follows: 12 images before the earthquake were downloaded within the period of 10th–21st February 2005. In addition, one image was downloaded during the earthquake on 22nd February 2005, and six more images after the earthquake were downloaded for the period of February 23th–28th 2005.

The same data before, during, and after the earthquake for 2005 were used for the years 2004 and 2007. Hence, in the current study, the data for one year before the earthquake (2004) and two years after the earthquake (2007) were considered as well. The MODIS satellite data for both 2004 and 2007 were downloaded from the same source as for 2005. So, 19 images were considered for 2004 and 2007

from February 10th to 28th. The same data was also downloaded for the 10th to 28th for 2007 and compared to 2005 to indicate that the temperature anomaly was due to the earthquake. The air temperature was also used to show the increase in air temperature during the earthquake. Therefore, the air temperature for February 2005 was downloaded for the whole month. Air temperature for 2004 and 2007 were also used to compare with 2005. So, to measure the air temperature, the average of ten years before since 1994–2004, and six years after the earthquake since 2006–2011, compared with 2005 as background.

### 3.3 Detection of LST Variation

Detection of thermal anomalies has been described by Wan and Dozier [37]. In this technique, they used a split window and some statistical techniques to calculate thermal anomalies. Fortunately, MODIS has a product of LST, which can be used for research in order to indicate LST variation. Therefore, this study uses MODIS satellite LST data to indicate LST variation during the earthquake. As explained in the previous section, after downloading the images, the data were processed: first, pre-processing, the MODIS LST data have already been pre-processed. Secondly, the LST product data should be converted to LST in Kelvin and then Celsius. So, the first step is to convert LST data to Kelvin. In order to do this conversion, the LST data should be multiplied by a scale factor of 0.02. Hence, the conversion of LST data to Kelvin has been used (Eq. 1):

$$LST (K) = RD * 0.02 \quad (1)$$

where,  $LST (K)$  is the land surface temperature in Kelvin,  $RD$  is the raw data of MODIS LST, and 0.02 is the scale factor.

Remote sensing software like ENVI was used to convert the first equation. The LST data in Kelvin was achieved through this conversion. Therefore, for this purpose, LST Kelvin was subtracted from 273. Then, all values have been changed to Celsius. Therefore, the conversion equation is given as Eq. (2):

$$LST (°C) = LST (K) - 273 \quad (2)$$

where,  $LST (°C)$  is  $LST$  data in Celsius.

In order to indicate the growth of the thermal anomaly, the LST data in Celsius were transferred to ArcGIS software to show LST variation during the earthquake. Therefore, the data were transferred to ArcGIS 10.2. Then, the data was divided into nine classes using the symbology function. Finally, the data was exported and saved as a final LST map, so the variation of LST can be easily observed. The flow chart of this research is shown in Fig. 2.

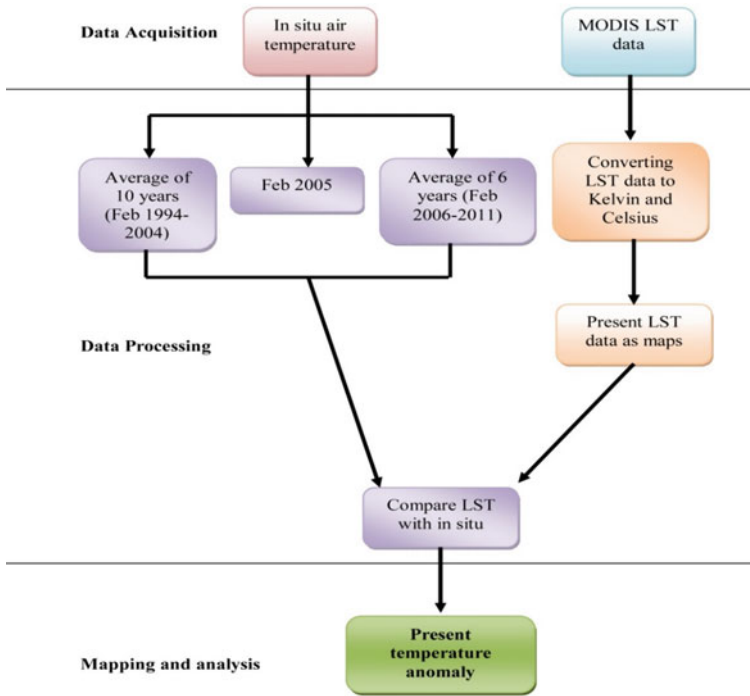


Fig. 2 Flow chart of research methodology adopted in this study

## 4 Results and Discussion

### 4.1 LST Variation Prior to Earthquake for 2005

The results of the MODIS daytime series LST maps from 10 to 28th February 2005 are provided in Fig. 3. The LST maps show a thermal anomaly that appeared before the devastating Zaran earthquake, which occurred on 22nd February 2005. The LST maps show that the LST on 16th February was 28 °C, while on 21st February it was 37 °C. Therefore, there was an LST difference of about 9 °C between both dates (Fig. 3). At some places, the LST was about 6–10 °C higher than the usual temperature in that period. In the daytime maps, it can be seen that before 15th February 2005, the LST in the region was indeed at the normal level. The development of a thermal anomaly around the earthquake epicenter started from 16th February 2005 and peaked on 21st February 2005, a day before the earthquake. After experiencing a thermal anomaly of about 5–9 °C, the LST in the region recovered to normal conditions on 25th February 2005 (Fig. 3).

The investigation of pre- and post-earthquake thermal anomalies by analyzing LST images has shown valuable information about changes in the TIR regime of the affected area. The analysis of the time series of the LST maps from 10 to 28th

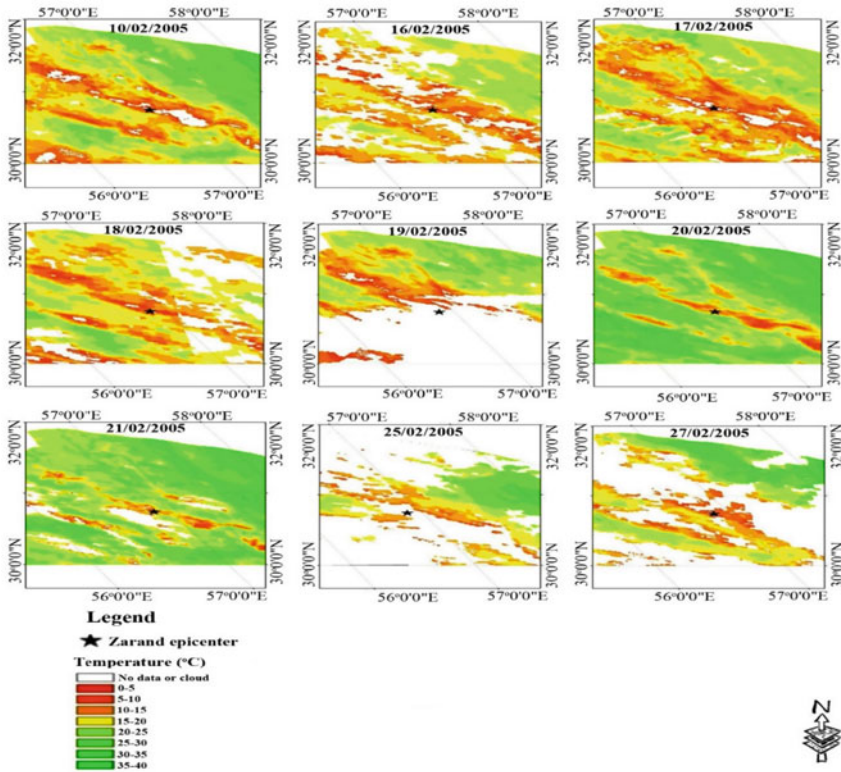


**Fig. 3** MODIS day time series LST maps since 10th–28th February 2005; white region indicates no data or cloud

February 2005 showed that anomalies started six days before the main shock. This anomalous LST region increases spatially and in intensity (Fig. 3). The results of this study are in line with previously published works including Choudhury et al. [38], Kancherla et al. [27], and Saraf et al. [22].

Panda et al. [31] analyzed the daytime MODIS LST product to the investigation of obtained LST and occurred Kashmir earthquake. The anomaly started to develop to the south-west of the epicenter and spread out to a large area with LST of 37–44 °C. The earthquake occurred on 8th October 2005. On 7th October 2005, just one day before the earthquake, the epicentral region experienced its highest temperature, which was around 4–8 °C different. In this study, during the Zarand earthquake the peak temperature was seen before the earthquake, and the thermal anomaly started six days before the earthquake.

As a matter of fact, one of the causes of LST anomalies is tectonic stresses. It is known that an increase in rock pressure leads to an increase in temperature.



## 4.2 Correlation Between MODIS LST and In-Situ Air Temperature

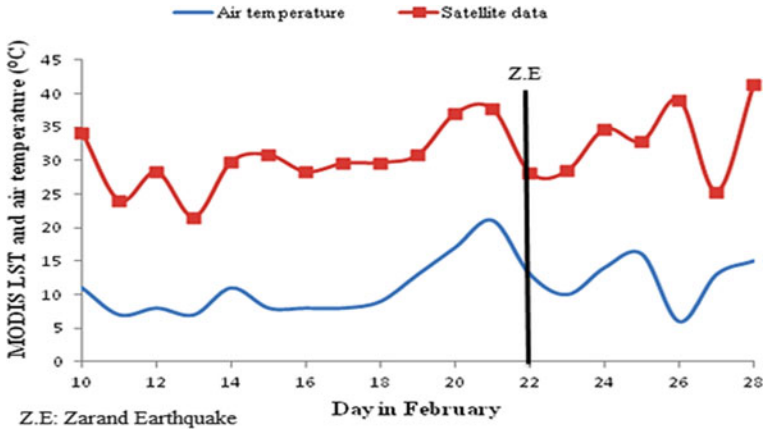
The LST retrieved from the MODIS thermal infrared sensor was compared with in-situ air temperatures observed on the same dates. The MODIS LST and maximum air temperature data are listed in Table 1.

Table 1 shows the correlation between the MODIS LST and in-situ air temperatures from the 10th to 28th February 2005. To better understand the variations of LST and air temperature, they are graphically presented as mentioned in Fig. 4. As shown in Fig. 4, the MODIS-retrieved LST agreed well with the ground observation of air temperature. Interestingly, both LST and air temperature started to increase from 16th February and both also peaked on 21st February 2005.

As can be seen in Fig. 4, the air temperature for day 15th–17th February was around 8 °C, which started to rise gradually. A surface air temperature of 17 °C was recorded on 20th February 2005. Also, the region experienced its maximum rise in air temperature on 21st February 2005, which was 4–8 °C higher than the temperature of the previous days (19th–21st February), while the MODIS LST increased about 1–7 °C compared to that during the period of 19th–21st February.

**Table 1** MODIS LST and in-situ air temperature data

Dates of February 2005	In-situ air temperature	MODIS LST
10	11.0	34.1
11	7.0	24.0
12	8.0	28.2
13	7.0	21.5
14	11.0	29.8
15	8.0	30.8
16	8.0	28.2
17	8.0	29.5
18	9.0	29.6
19	13.0	30.8
20	17.0	37.0
21	21.0	37.0
22	13.0	28.1
23	10.0	28.4
24	14.0	34.6
25	16.0	32.8
26	6.0	39.0
27	13.0	25.3
28	15.0	41.4



**Fig. 4** Variation of MODIS LST and in-situ air temperature before and after the Zarand earthquake within the period from 10 to 28th February 2005. The black bar indicates the date of the Zarand earthquake

The MODIS LST on the 19th was 30.8 °C, while on 21st February, the temperature rose to 37 °C (Fig. 4). As is clear in Table 2 and Fig. 4, the MODIS LST reached a maximum on 21st February with the temperature of 37 °C, but on 22nd February a lower temperature was recorded. 28 °C was recorded for the MODIS LST and 13 °C for air temperature for 22nd February 2005. After the 21st, both the MODIS LST and air temperature continued to decrease until 23rd February, and then both air temperature and the MODIS LST showed small increases on the 25th, which was 16 °C for air temperature and 32 °C for the MODIS LST.

### 4.3 Comparisons of 2005 LST with 2004 and 2007 LSTs

In order to ensure whether the increase in MODIS LST from 16th February 2005 was associated with the Zarand earthquake, the same analysis was also conducted for the years 2004 and 2007 within the same period (10th to 28th February). Furthermore, compared to the year 2005, there was no unusual MODIS LST increase which started from 16th February in both years 2004 and 2007 (Fig. 5).

Overall, the MODIS LST was in its normal condition in both 2004 and 2007. The MODIS LST for the years 2004, 2005, and 2007 are shown in Table 2. As can be seen in Table 2, for 2005 the peak temperature was recorded on 21st February at 41.6 °C. This is the maximum value for this year in the period of 19 days from 10 to 28th February. In order to compare 21st February 2005 with the previous year, i.e. 2004, the LST recorded was 34.6 °C, which is 7 °C lower than 2005. On the 21st February 2007, the LST was 37.3 °C, which is 4 °C lower than on 21st February 2005. In addition, in 2005 within the period of 16th–22nd February, the MODIS LST

**Table 2** MODIS LST for the years 2004, 2005, and 2007

Day	Year 2004	Year 2005	Year 2007
10	36.5	34.1	35.0
11	38.5	24.0	36.4
12	37.6	28.2	35.6
13	40.5	21.5	34.8
14	42.3	29.8	36.4
15	44.0	30.8	33.3
16	37.8	28.2	40.0
17	33.7	29.5	38.6
18	40.3	29.6	37.4
19	41.6	30.8	36.8
20	39.5	37.0	36.6
21	34.6	41.6	37.3
22	40.0	28.1	32.2
23	37.0	28.4	36.3
24	35.8	34.6	35.2
25	40.8	32.8	43.7
26	41.0	39.0	35.9
27	42.7	25.3	30.7
28	40.4	41.4	36.4

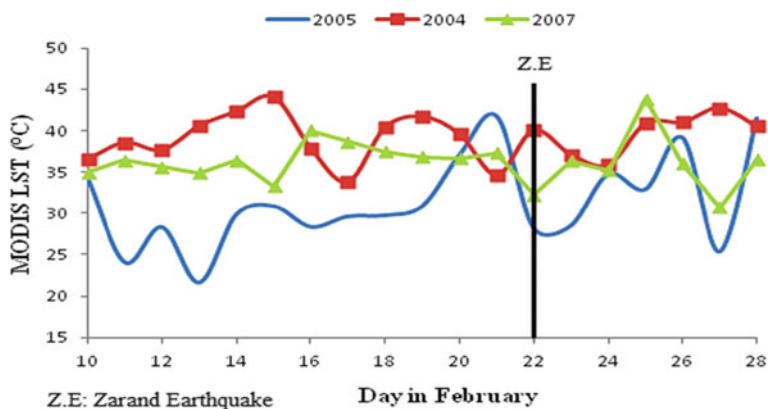


**Fig. 5** MODIS LST variation for the years 2004, 2005, and 2007. The black bar indicates the date of the Zarand earthquake

increased gradually from 28 to 41 °C, while in the previous year the same increase cannot be seen. For 2004, within the 16th–22nd February period, the LST values were 33–40 °C (Table 2).

In order to better understand the MODIS LST for the years 2004, 2005, and 2007, they are presented in Fig. 5. Furthermore, the time series LST maps for the years 2004 and 2007 are provided for the period of 10th–28th February in order to compare with 2005. In 2005, the thermal anomaly started to increase from 6th–21st February, while no such thermal anomaly was observed in the years 2004 and 2007 (Fig. 6).

Research has been done by Saraf and Choudhury [21] into an earthquake in Bhuj, Gujarat, India. The earthquake occurred on 26th January 2001. In this research, thermal channels were used to calculate LST over the study area. The LST maps over the region have been provided to indicate the thermal anomaly. The data from the year 2003 from the same region and same dates were also used to study the LST situation and compare between LST in 2001, when the earthquake occurred, and 2003, two years after the earthquake. It was seen that in 2003 there was a completely normal thermal scenario in and around the epicenter. This research shows that the increasing thermal anomaly in 2001 was due to the earthquake and there was no such thermal anomaly in 2003.

#### ***4.4 Air Temperature Anomaly***

The in-situ air temperature data for the whole month of February were analyzed to understand the correlation between earthquake events and the air temperature variation. The air temperature data from the Zarand meteorological stations are available from the daily climate and weather data statistics website. The maximum temperature values were plotted against the dates within the period 1st–28th February. The maximum air temperature variation for February 2005 was compared with the normal air temperature (generated from ten years of data from 1994 to 2004, and six years from 2006 to 2011—Fig. 7).

The air temperature in Zarand showed a rise of around 4 °C on 19th February 2005 and 5.5 °C on 20th February 2005 with respect to the mean normal air temperature (Fig. 7). On 22nd February 2005, the air temperature deviated as high as 7.5 °C from the normal air temperature, and on 26th February 2005, it was almost the same as that of normal conditions. Although the magnitude of the in-situ air temperature is lower than MODIS LST, the observed in-situ air temperature variation supported the LST variation observed by MODIS, showing that the thermal anomaly seemed to occur a few days before the earthquake and dissipated after the earthquake, which agreed well with previous results [31].

The difference between the in-situ air temperature magnitudes and MODIS LST is normal as the instrument used to measure in-situ air temperature is usually placed at 1.5 m above the ground [22]. Furthermore, the LST obtained from MODIS is the surface skin temperature estimated from the Earth's emission [21]. The in-situ air temperature data from the daily climate weather data statistics website for the year

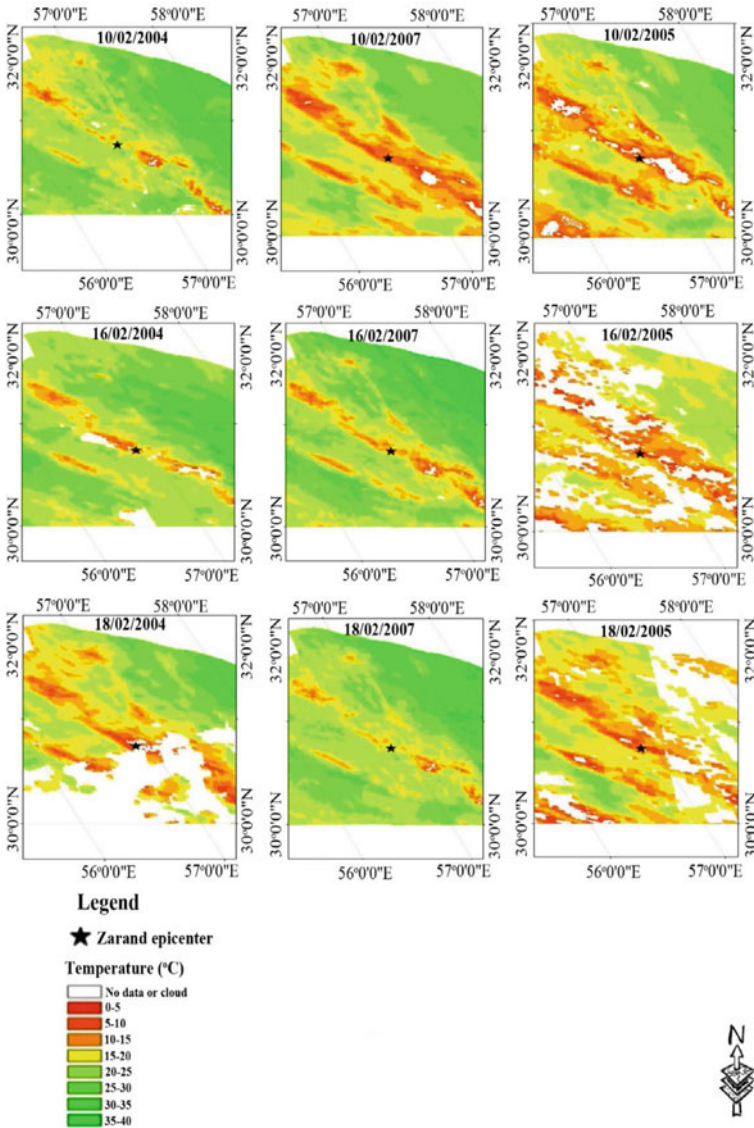


**Fig. 6** a Time series of LST maps for years 2004 and 2007 to be compared with 2005 (9 days). b Time series of LST maps for 2004 and 2007 to be compared 2005 (another 9 days)

2005 and the average of 10 years before the earthquake (1994–2004) and six years after the earthquake (2006–2011) are listed in Table 3.

Furthermore, before the earthquake on 21st February 2005, there was an increase in air temperature of 4–6 °C, which did not occur in 2004 and 2007. From 1st February to 10th February in 2004, 2005, and 2007, the in-situ air temperature showed similar

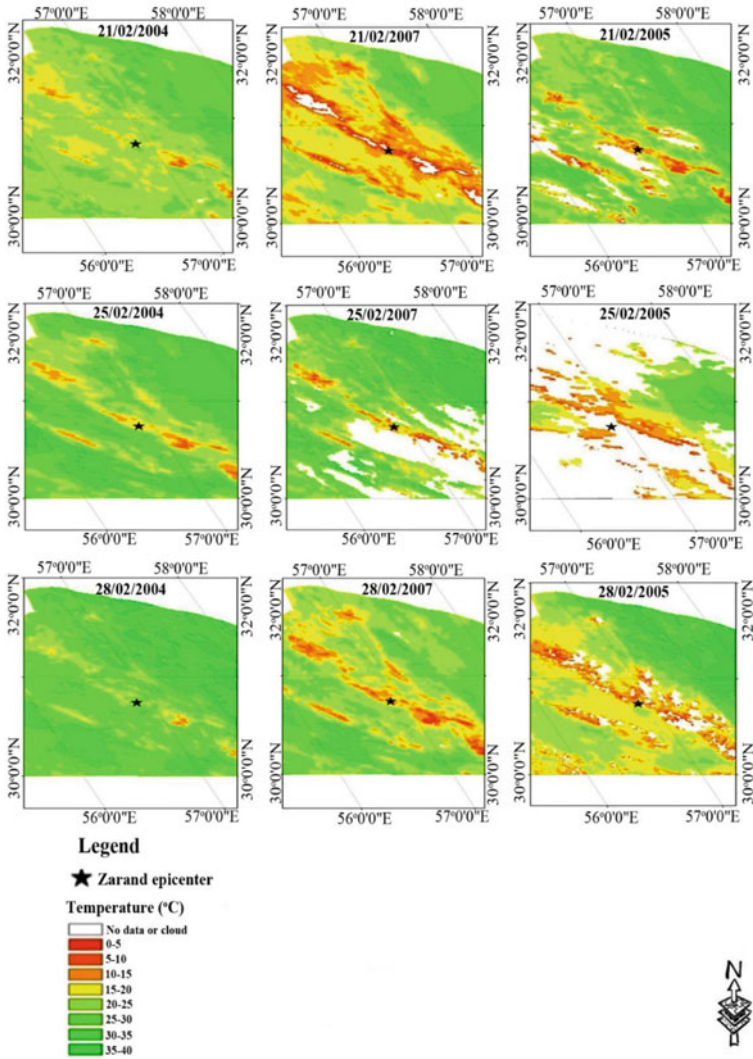
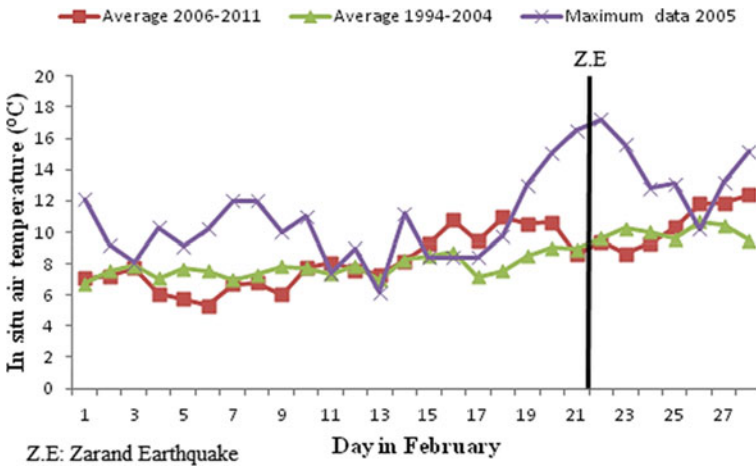


Fig. 6 (continued)

patterns. From 16th February the air temperatures started to rise from 8 to 21 °C on 21st February. After 21st February, the temperature decreased and on 24th February, the temperature relaxed to the normal condition (Fig. 8).



**Fig. 7** Temporal variation of in-situ air temperature collected at Zarand meteorological station for the year 2005 (maximum temperature), and mean of average values for the years 2006 to 2011 and the years 1994 to 2004. The black bar indicates the date of the Zarand earthquake

## 5 Conclusions

The Zarand earthquake in Kerman Province in central Iran triggered numerous geo-hazards, including landslides, rock avalanches, and debris flows. These geo-hazards caused heavy losses by destroying roads, burying villages, blocking rivers and damaging vegetation. It is noted that MODIS Terra thermal data sets have been confirmed to be valuable in successfully detecting earthquake thermal anomalies. The analysis of MODIS daytime LST and in-situ air temperature data for the whole month of February 2005 reveals a distinct, robust, and rapid rise in LST before the Zarand earthquake. The affected region may take days to weeks to attain normal temperature conditions after the main event.

As successfully demonstrated in the present study to analyze LST variation for 2005, the Zarand earthquake was associated with pre-earthquake thermal anomalies. The anomalies appeared six days before the earthquake. The increase in temperature ranges between 5 and 10 °C. The MODIS LST data for 2004 and 2007 data were also analyzed from 10th to 28th and compared to those of 2005, since there is no temperature variation in 2004 and 2007. The LST maps indicated normal conditions in 2004 and 2007, with no thermal anomaly, such as that seen in 2005. The analysis relates to the observational study for the detection of pre-earthquake anomalies, and it provides an understanding of the pattern of growth for TIR anomalies and may assist in the development of a reliable potential earthquake thermal precursor. Besides, regarding the air temperature, a pattern of growth has been observed in 2005. In-situ air temperature, like LST, has indicated growth before and during the earthquake.

**Table 3** Maximum of in-situ air temperature data for 2005 and mean of air temperature for the years 1994–2004 and 2006–2011, collected from Zarand meteorological stations

Date	Mean values 2006–2011	Mean values 1994–2004	Maximum values 2005
1	7.1	6.7	12.1
2	7.2	7.5	9.2
3	7.7	7.9	8.1
4	6.1	7.0	10.3
5	5.7	7.6	9.1
6	5.3	7.5	10.2
7	6.7	6.9	12.0
8	6.7	7.3	12.0
9	6.0	7.8	10.0
10	7.7	7.7	11.0
11	8.1	7.3	7.4
12	7.6	7.9	9.0
13	7.3	6.9	6.2
14	8.1	8.2	11.2
15	9.2	8.5	8.4
16	10.8	8.7	8.4
17	9.4	7.1	8.4
18	10.9	7.5	9.8
19	10.5	8.5	13.0
20	10.6	9.0	15.1
21	8.5	8.9	16.5
22	9.3	9.6	17.2
23	8.6	10.2	15.6
24	9.3	10.0	12.8
25	10.2	9.5	13.1
26	11.8	10.6	10.2
27	11.8	10.4	13.2
28	12.3	9.4	15.2

## 6 Recommendations

It is noted that the remote sensing missions in the future have an important role in calculating LST before each earthquake in the world. The new satellites with equipment sensors in better spatial, spectral, and radiometric resolutions can detect more anomalies before occurring of an earthquake.

For example, in optical remote sensing, Landsat 9 will be equipped with the Thermal Infrared Sensor 2 (TIRS-2) to provide the LST and act as an upgraded version of the Landsat 8 TIRS instrument by solving the known stray light and



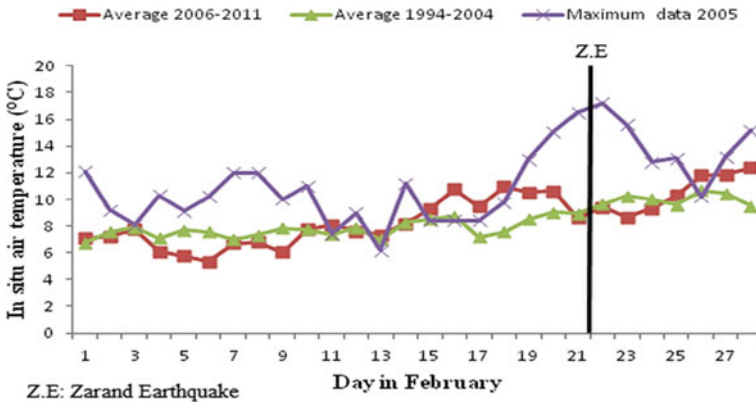


**Fig. 8** Temporal variation of maximum in-situ air temperature collected at Zarand meteorological station for 2004, 2005, and 2007. The black bar indicates the date of the Zarand earthquake

reliability issues with the TIRS. Furthermore, in radar remote sensing, Sentinels 4, 5, and Sentinel-5P with orbits of geostationary and sun-synchronous can detect and measure the omitted surface temperature with more precision. Finally, although the prediction of earthquakes in the present time is impossible but more research on the earthquakes in different geographical locations by the advanced equipment in remote sensing data can predict an earthquake precisely and on time.

## References

1. Symeonakis E, Karathanasis N, Koukoulas S, Panagopoulos G (2016) Monitoring sensitivity to land degradation and desertification with the environmentally sensitive area index: the case of Lesbos island. *Land Degrad Dev* 27:1562–1573
2. Taheri K, Shahabi H, Chapi K, Shirzadi A, Gutiérrez F, Khosravi K (2019) Sinkhole susceptibility mapping: a comparison between Bayes-based machine learning algorithms. *Land Degrad Dev* 30:730–745
3. Alizadeh M, Alizadeh E, Asadollahpour Kotenaee S, Shahabi H, Beiranvand Pour A, Panahi M, Bin Ahmad B, Saro L (2018) Social vulnerability assessment using artificial neural network (ANN) model for earthquake hazard in Tabriz city, Iran. *Sustainability* 10:3376
4. Lee S, Panahi M, Pourghasemi HR, Shahabi H, Alizadeh M, Shirzadi A, Khosravi K, Melesse AM, Yekrangnia M, Rezaie F (2019) Sevucas: a novel gis-based machine learning software for seismic vulnerability assessment. *Appl Sci* 9:3495
5. Wang Y, Hong H, Chen W, Li S, Panahi M, Khosravi K, Shirzadi A, Shahabi H, Panahi S, Costache R (2019) Flood susceptibility mapping in Dingnan County (China) using adaptive neuro-fuzzy inference system with biogeography based optimization and imperialistic competitive algorithm. *J Environ Manage* 247:712–729
6. Shahabi H, Shirzadi A, Ronoud S, Asadi S, Pham BT, Mansouripour F, Geertsema M, Clague JJ, Bui DT (2021) Flash flood susceptibility mapping using a novel deep learning model based on deep belief network, back propagation and genetic algorithm. *Geosci Front* 12:101100

7. Jaafari A, Zenner EK, Panahi M, Shahabi H (2019) Hybrid artificial intelligence models based on a neuro-fuzzy system and metaheuristic optimization algorithms for spatial prediction of wildfire probability. *Agric For Meteorol* 266:198–207
8. Oliveira S, Gonçalves A, Zêzere JL (2021) Reassessing wildfire susceptibility and hazard for mainland Portugal. *Sci Total Environ* 762:143121
9. Nefeslioglu HA, Tavus B, Er M, Ertugrul G, Ozdemir A, Kaya A, Kocaman S (2021) Integration of an InSAR and ANN for sinkhole susceptibility mapping: a case study from Kirikkale-Delice (Turkey). *ISPRS Int J Geo Inf* 10:119
10. Mokarram M, Pourghasemi HR, Hu M, Zhang H (2021) Determining and forecasting drought susceptibility in southwestern Iran using multi-criteria decision-making (MCDM) coupled with CA-Markov model. *Sci Total Environ* 781:146703
11. Van Dao D, Jaafari A, Bayat M, Mafi-Gholami D, Qi C, Moayedi H, Van Phong T, Ly H-B, Le T-T, Trinh PT (2020) A spatially explicit deep learning neural network model for the prediction of landslide susceptibility. *CATENA* 188:104451
12. Arabameri A, Cerda A, Pradhan B, Tiefenbacher JP, Lombardo L, Bui DT (2020) A methodological comparison of head-cut based gully erosion susceptibility models: combined use of statistical and artificial intelligence. *Geomorphology* 359:107136
13. Bhattacharya RK, Das Chatterjee N, Das K (2021) Land use and land cover change and its resultant erosion susceptible level: an appraisal using RUSLE and logistic regression in a tropical plateau basin of West Bengal, India. *Environ Dev Sustain* 23:1411–1446
14. Ebrahimi H, Feizizadeh B, Salmani S, Azadi H (2020) A comparative study of land subsidence susceptibility mapping of Tasuj plane, Iran, using boosted regression tree, random forest and classification and regression tree methods. *Environ Earth Sci* 79:1–12
15. Mosavi A, Hosseini FS, Choubin B, Abdolshahnejad M, Gharechae H, Lahijanzadeh A, Dineva AA (2020) Susceptibility prediction of groundwater hardness using ensemble machine learning models. *Water* 12:2770
16. Maqsoom A, Aslam B, Awais M, Hassan U, Alaloul WS, Musarat MA, Qureshi MI (2021) Efficiency of multiple hybrid techniques for the earthquake physical susceptibility mapping: the case of Abbottabad District, Pakistan. *Environ Earth Sci* 80:1–20
17. Lu X, Meng Q, Gu X, Zhang X, Xie T, Geng F (2016) Thermal infrared anomalies associated with multi-year earthquakes in the Tibet region based on China's FY-2E satellite data. *Adv Space Res* 58:989–1001
18. Li, J, Liu C, Zheng Y, Xiong X (2017) Rupture process of the M<sub>s</sub> 7.0 Lushan earthquake determined by joint inversion of local static GPS records, strong motion data, and teleseismograms. *J Earth Sci* 28:404–410
19. Tramutoli V, Cuomo V, Filizzola C, Pergola N, Pietrapertosa C (2005) Assessing the potential of thermal infrared satellite surveys for monitoring seismically active areas: the case of Kocaeli (Izmit) earthquake, August 17, 1999. *Remote Sens Environ* 96:409–426
20. Ouzounov D, Freund F (2004) Mid-infrared emission prior to strong earthquakes analyzed by remote sensing data. *Adv Space Res* 33:268–273
21. Saraf A, Choudhury S (2005) Cover: satellite detects surface thermal anomalies associated with the Algerian earthquakes of May 2003. *Int J Remote Sens* 26:2705–2713
22. Saraf AK, Rawat V, Das J, Zia M, Sharma K (2012) Satellite detection of thermal precursors of Yamnotri, Ravar and Dalbandin earthquakes. *Nat Hazards* 61:861–872
23. Tronin A, Biagi P, Molchanov O, Khatkevich Y, Gordeev E (2004) Temperature variations related to earthquakes from simultaneous observation at the ground stations and by satellites in Kamchatka area. *Phys Chem Earth Parts A/B/C* 29:501–506
24. Carreno E, Capote R, Yague A, Tordesillas J, Lopez M, Ardizzone J, Suarez A, Lzquierdo A, Tsige M, Martinez J (2001) Observations of thermal anomaly associated to seismic activity from remote sensing. General Assembly of European Seismology Commission, Portugal, p 269
25. Tronin AA, Hayakawa M, Molchanov OA (2002) Thermal IR satellite data application for earthquake research in Japan and China. *J Geodyn* 33:519–534

26. Ouzounov D, Liu D, Chunli K, Cervone G, Kafatos M, Taylor P (2007) Outgoing long wave radiation variability from IR satellite data prior to major earthquakes. *Tectonophysics* 431:211–220
27. Kancherla VK, Mandla VR, Arrowsmith C (2018) Study of thermal IR phenomena associated with 27 February 2010 Chile Mw 8.8 earthquake using MODIS data. *Geocarto Int* 33:293–309
28. Liu C, Zheng Y, Xiong X (2015) Focal mechanism and rupture process of the 2012 Mw 7.0 Santa Isabel, Mexico earthquake inverted by teleseismic data. *J Earth Sci* 26:384–390
29. Lü Q-Q, Ding J-H, Cui C-Y (2000) Probable satellite thermal infrared anomaly before the Zhangbei M<sub>s</sub>= 6.2 earthquake on January 10, 1998. *Acta Seismologica Sinica* 13:203–209
30. Qin X, Tan C, Chen Q, Wu M, Feng C (2014) Crustal stress state and seismic hazard along southwest segment of the Longmenshan thrust belt after Wenchuan Earthquake. *J Earth Sci* 25:676–688
31. Panda S, Choudhury S, Saraf A, Das J (2007) MODIS land surface temperature data detects thermal anomaly preceding 8 October 2005 Kashmir earthquake. *Int J Remote Sens* 28:4587–4596
32. Pulinet S, Ouzounov D, Karelin A, Boyarchuk K, Pokhmelnikh L (2006) The physical nature of thermal anomalies observed before strong earthquakes. *Phys Chem Earth Parts A/B/C* 31:143–153
33. Ahmadian J, Murata M, Nadimi A, Ozawa H, Kozai T (2014) Active tectonics of Iran deduced from earthquakes, active faulting, and GPS evidence. *Bull Cent Collab Comm Naruto Univ Edu* 28:11–22
34. Talebian M, Jackson J (2002) Offset on the main recent fault of NW Iran and implications for the late Cenozoic tectonics of the Arabia-Eurasia collision zone. *Geophys J Int* 150:422–439
35. Xiong X, Wolfe R, Barnes W, Guenther B, Vermote E, Saleous N, Salomonson V (2010) Terra and Aqua MODIS design, radiometry, and geometry in support of land remote sensing. In: *Land remote sensing and global environmental change*. Springer, pp 133–164
36. Roodposhti MS, Safarrad T, Shahabi H (2017) Drought sensitivity mapping using two one-class support vector machine algorithms. *Atmos Res* 193:73–82
37. Wan Z, Dozier J (1996) A generalized split-window algorithm for retrieving land-surface temperature from space. *IEEE Trans Geosci Remote Sens* 34:892–905
38. Choudhury S, Dasgupta S, Saraf AK, Panda S (2006) Remote sensing observations of pre-earthquake thermal anomalies in Iran. *Int J Remote Sens* 27:4381–4396